DOI 10.1007/s10553-024-01731-9
Chemistry and Technology of Fuels and Oils, Vol. 60, No.3, July, 2024 (Russian Original No.3, May – June, 2024)

INNOVATIVE TECHNOLOGIES OF OIL AND GAS

CHARACTERIZATION OF PORE STRUCTURE AND TWO-PHASE SEEPAGE PATTERN IN SANDSTONE CONGLOMERATE BASED ON CT SCANNING

Zhang Jing[1,2] ✉, Liu Canhua[2], Dong Guangtao[3], Dong Yan[2], Zhou Fujian[1]

Oil and gas occurrence characteristics and seepage characteristics of tight reservoirs are the key to production. CT technology can monitor displacement and advance seepage front in time In this chapter, NMR experiments of spontaneous imbibition and CT monitoring experiments of differential pressure displacement are carried out for dense conglomerate to clarify the law of two-phase seepage. The results show that in spontaneous imbibition, the fluid circulation in the pore of tight glutenite is high, and there is no micro-fracture The pore volume of clay minerals with high content increases when exposed to water, which improves the imbibition recovery ratio However, the highly heterogeneous gravel distribution increases the complexity of seepage path and thus enhances the imbibition recovery ratio. The strong heterogeneity of sandy conglomerate leads to the formation of preponderant passages in seepage In the early stage of displacement, the water flooding effect is poor and a large amount of water accumulates With the increase of displacement time, there is no obvious change in oil saturation at both ends of the middle part of a large number of water rock samples The oil saturation is lower at both ends and higher in the middle.

Keywords: tight reservoirs, two-phase seepage, imbibition recovery ratio, tight glutenite, oil saturation.

1. Introduction

The oil and gas storage characteristics and seepage characteristics of tight reservoirs are the key to production, and the oil and gas storage characteristics include the distribution characteristics of crude oil in reservoirs and the distribution characteristics of post-production residual oil, and the main factors affecting the storage space include the rock structure, mineral composition, sedimentary diagenesis, physical characteristics, pore throat characteristics, and the content of organic matter [1]. Currently, fluorescence analysis, field scanning electron microscopy (FSE), centrifugal nuclear magnetic resonance (NMR) and molecular dynamics simulation [2] are commonly used.

---

[1] Unconventional Petroleum Research Institute, China University of Petroleum, Beijing, China; [2] Research Institute of Exploration and Development, Xinjiang Oilfield Company, PetroChina, Karamay, China; [3] State Key Laboratory for Geomechanics and Deep Underground Engineering, China; University of Mining and Technology (Beijing), Beijing, China. *Corresponding author: Zhang Jing ✉. E-mail: xiaohengchinapetro@163.com.* Translated from *Khimiya i Tekhnologiya Topliv i Masel*, No. 3, pp. 184–189, May – June, 2024.

The residual oil is usually analyzed by fluorescence analysis, which can be classified into free, semi-bound and bound states according to the states of water and residual oil in the pore space [3]. Under the scanning electron microscope (SEM), there are three kinds of oil states, namely free state, dissolved state and adsorbed state [4]. Under centrifugal nuclear magnetic resonance (NMR), the saturation of movable fluid increases with the increase of permeability, and the mobilized space mainly comes from the macro-porous [5]. At present, the numerical simulation of oil-bearing storage is mainly molecular dynamics simulation, which can investigate the proportion of oil in different storage states and the movement law of storage paths, and can be used to estimate the reservoir resources [6].

The development effect of tight reservoirs is usually affected by both capillary force seepage efficiency and displacement efficiency. Seepage is an effective method to exploit the pore space crude oil in tight oil and gas reservoirs, and the driving fluid has wettability, while the driving fluid has no wettability. Usually, the factors affecting seepage include permeability, mineralization, viscosity ratio, temperature, interfacial tension, porosity, wetting angle and fracture width, etc. [7, 8]. In addition, boundary conditions are also one of the important factors affecting the efficiency of seepage. The five boundary conditions include full contact seepage, top closed seepage, bottom closed seepage, side closed seepage, and top-bottom closed seepage, among which the top-bottom closed seepage has the highest recovery rate and the side closed seepage has the lowest recovery rate [9]. Only reverse seepage exists at the single boundary, and both isotropic and reverse seepage exist at the mixed boundary [10].

The seepage process is mainly affected by capillary force and gravity, and NB -1 can be used to distinguish the dominant position of capillary force or gravity in the seepage process [11]. When NB -1 is greater than 1, capillary force plays a dominant role, and oil and water are replaced in the reverse direction; NB-1 is less than 1, gravity plays a dominant role, and oil and water are replaced in the same direction [12]. The traditional seepage test method is mainly the weighing method, which analyzes the seepage law by mass or volume change, and the current experiments on seepage mostly use nuclear magnetic resonance technology, CT technology, microscopic visualization experiments, neutron scattering imaging, etc. [13, 14]. Domestic and foreign scholars have proposed many matching models for the seepage phenomenon, including LW model, Terzaghi model, Handy model, and also established spontaneous seepage scalar model, unfactored time and normalized recovery rate, etc. Numerical simulation of spontaneous seepage is currently in progress. Numerical simulations of spontaneous seepage are mainly pore network simulations, computational fluid dynamics methods, finite element methods, lattice Boltzmann methods, and molecular dynamics simulations [15]. At present, in the study of spontaneous seepage in gravel, how to establish a reasonable model of spontaneous seepage is still to improve the accuracy [16].

In reservoir recovery, displacement usually refers to the process of replacing oil in pores or fractures by injecting fluids at constant flow under applied temperature and pressure. Currently, the main types of replacement include water drive, gas drive, foam drive, polymer drive and chemical drive. Water drive is the main form of oilfield exploitation, adjusting the injection rate and pressure can flexibly improve the recovery rate, but this type of exploitation has certain shortcomings, affecting the efficiency of oil drive more factors, including macro non-homogeneity and micro-pore structure. For reservoirs with strong water sensitivity, water drive will lead to the destruction of reservoir structure [17]. Gas drive refers to gas injection can form a mixed phase, can also reduce the interfacial tension, viscosity, thus increasing the range of wave, improve oil recovery, the disadvantage is that the cost of gas injection is high, prone to gas flurry, less applicable reservoirs [18]. Foam drive refers to the way of gas foam oil drive, gas-liquid contact to form foam can effectively block the throat, enhance the wave area, the disadvantage is that some of the gas is expensive, less gas source [19].

Polymer drive is mainly for the non-homogeneous reservoir water drive process refers to the phenomenon of the subsequent replacement method, this method can increase the viscosity of the water phase, spread the wave area, effectively prevent the water drive is easy to form the advantage of the channel, the disadvantage is that it becomes a high cost, research and development difficulties, low compatibility, and the application of the field to a long period of time [20]. For replacement experiments, NMR technology and CT technology are often used. Nuclear magnetic resonance technology can calculate the recovery rate and residual oil saturation [21], the seepage under capillary force comes from the matrix system, and the seepage under differential pressure comes from the fracture network, and there is no pore size distinction between the two [22]. CT technology can monitor the process of the replacement, and grasp the advancement process of the seepage leading edge in time. In addition, during the development

of replacement in gravel reservoirs, the phenomenon of fingering usually exists, and the pore variability and unconnected seepage channels can lead to low water injection recovery.

2. Experimental steps and methods

The porosity and permeability of dense conglomerate are very small, so the study of seepage characteristics often needs to be analyzed with the aid of high-resolution equipment, and this experiment relies on high-precision micrometer CT to monitor the microscopic replacement process of conglomerate on-line. The radiation source in the micron CT equipment can emit X-rays during the scanning process, and most of the X-rays can pass through the entire rock structure, and the intensity of the rays after passing through the rock structure has a very good correlation with the density of the rock. The CT value of the core can be obtained by obtaining the intensity data from different angles and at different times in an efficient and fast way, and the CT value can be calculated by the following formula.

$$CT = \frac{\mu - \mu_w}{\mu_w} \cdot 1000,$$

where μ is the attenuation coefficient of the rock sample measured in the test and μ_w is the attenuation coefficient of the calibrated fluid (water).

Based on the scanned CT data, porosity and oil saturation calculations can be performed. CT calculations for dry rock samples and samples fully saturated with oil are shown below.

$$CT_{dry} = (1-\varphi)CT_{grain} + \varphi_i CT_{air},$$
$$CT_{wet} = (1-\varphi_i)CT_{grain} + \varphi_i CT_{water}.$$

By combining the above equations, the porosity of the core can be solved as follows.

$$\varphi_i = \frac{CT_{wet} - CT_{dry}}{CT_{water} - CT_{air}} \cdot 100\%.$$

During the replacement process, since the oil content of the pore space is decreasing and the water content is increasing, the pore space is still completely filled with fluid, so the saturation is still 100%, which is expressed by the following equation:

$$S_{oil} + S_{water} = 1.$$

When a certain replacement time, its internal oil and water coexistence, so the pore part of the CT value changes, then the whole core CT can be expressed by the following formula.

$$CT_t = (1-\varphi_i) + \varphi_i (S_{oil} CT_{oil} + S_{water} CT_{water}).$$

Combined equations to solve for oil saturation and water saturation variations:

$$S_{oil} = \frac{CT_{dry} - CT_t}{CT_{water} - CT_{oil}} \cdot \frac{CT_{water} - CT_{air}}{CT_{wet} - CT_{dry}} \cdot 100\%,$$

$$S_{water} = \left(1 - \frac{CT_{dry} - CT_t}{CT_{water} - CT_{oil}} \times \frac{CT_{water} - CT_{air}}{CT_{wet} - CT_{dry}}\right) \cdot 100\%,$$

where, CT_{dry} is the CT value of the dry rock sample; φ_i is the initial rock sample saturation; CT_{grain} is the CT value of the skeleton, due to the unavailability of, in the porosity and saturation calculations, around the CT value of the skeleton to eliminate the variable term; CT_{air} is the CT value of the air; CT_{wet} is the CT value of the rock sample after completely saturated with the fluid; CT_{water} is the CT value of air; S_{oil} is the oil saturation; S_{water} is the water saturation; CT_t is the CT value at a certain moment of expulsion.

In this experiment, the on-line seepage experiments of water-driven oil were carried out mainly on the samples of sand conglomerate, aiming to study the dynamic change characteristics of oil saturation in the process of displacement, which is influenced by the conglomerate, with strong non-homogeneity, and the pore structure of the conglomerate may have dominant channels. The specific experimental steps are as follows.

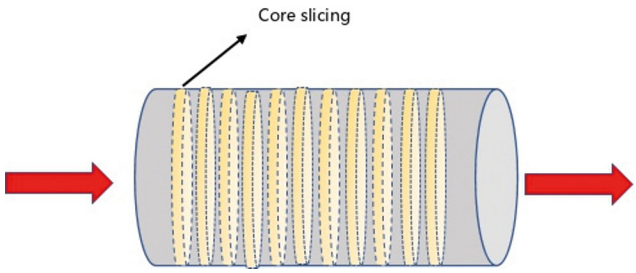

Fig. 1. Schematic diagram of scanning slice

Take conglomerate rock samples for cutting and processing, after washing, put them into the drying box at a temperature of 60° C for 24 hours. After taking out the dried rock samples, the samples were left to cool down to room temperature, and then put into the gripper to control the peripheral pressure of 15 MPa for CT scanning, and then vacuumed for 72 hours after the scanning.

After the end of vacuuming, saturate the formation water according to the formation pressure of 10 MPa, when the upstream and downstream pressures reach stability, at this moment the core system has reached the initial formation temperature and pressure state, and carry out a CT scanning to obtain the characteristics of the distribution of formation water in the rock as the initial state.

Gradient pressurization method was used to drive the rock samples to the state of bound water, and CT scanning was carried out when the oil phase flow rate was stabilized.

Afterwards, the rock samples were subjected to water drive treatment, the drive rate was set at 0.001 ml/min, and the cores were CT scanned at regular intervals.

When the water content at the outlet end of the drive exceeds 95% or more, the entire test process is completed.

The standard rock samples were selected for this experiment, and the samples were divided into several slices by CT scanning, as shown in **Figure 1**. Because the two ends of the rock samples were rough, there were more errors when importing them into the seepage analysis software, and therefore, when analyzing the slices in the statistical sectioning analysis, the first and the last ends of the sections were deleted, and the slices were totaled to be 42 slices.

3. Experimental results

Characterization of pore structure. As shown in **Figure 2**, the conglomerate sample MH-L1 has more primary intergranular pores, which are mainly formed by the aggregation of fillers under the sedimentary tectonics, and there are microcracks, with the width of cracks around 2 μm, and there are more mineral particles on the surface of the rock, mostly quartz particles with regular shape. Sample MH-L2 has more primary intergranular pores with high pore development. Sample MH-L3 has a small number of pores and small nanometer-sized cracks. Sample MH-L4 has a glossy surface, with a small number of pores, mostly small microcracks. Sample MH-L5 has more pores and poor surface roughness. Generally speaking, the gravels have more hard minerals such as quartz, and at the same time, there are more pores on the surface, and some samples have microcracks.

As shown in **Figure 3**, the mineral composition of the conglomerate is mainly quartz, with contents ranging from 36% to 43.2%, with an average of 36.9%. The clay minerals range from 25.4% to 42.4%, with an average of 32.32%. The high clay mineral content enhances the water sensitivity of the conglomerate. The feldspar minerals range from 2.6% to 28.4%, with an average of 19.72%. Among the clay minerals, the main component is immonite, with contents ranging from 13.5% to 68%, with an average of 44.2%, followed by kaolinite, with contents ranging from 4% to 71.2%, with an average of 24.6%. Some of the conglomerates have a very high kaolinite content, such as MH-L3, which has a kaolinite content of 71.2% and is very susceptible to hydration and expansion when exposed to water.

Porosity of the gravel cross-section. As shown in **Figure 4**, the water saturation of each slice is between 7.74% and 10.34%, and the average porosity is 9.37%. The difference between the measured porosity of water and the measured porosity of conglomerate is small, which indicates that the effect of pressurized saturated formation water is good, and it can be regarded as completely saturated. As shown in **Figure 5**, the distribution of pore fluid is not uniform, due to the presence of conglomerate,

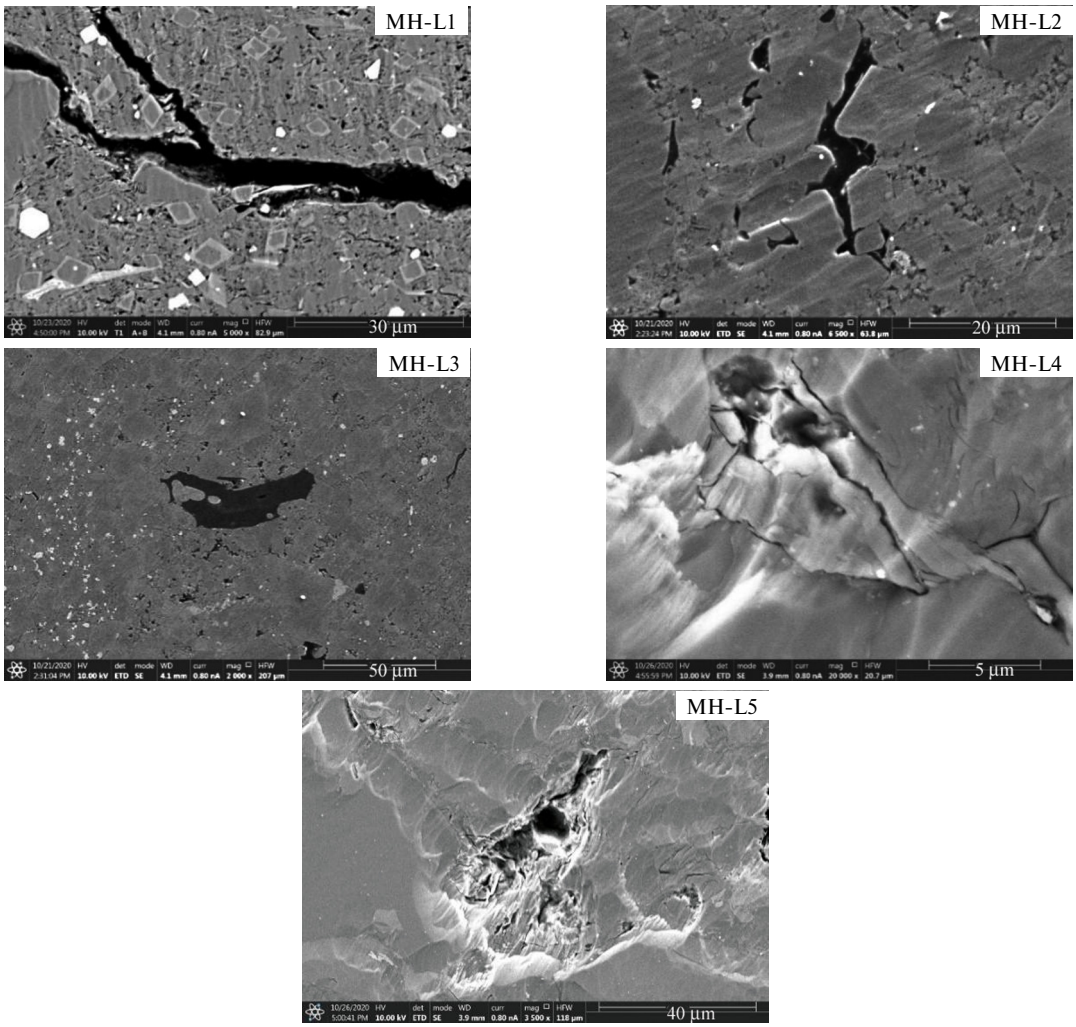

Fig. 2. SEM image of a sandy conglomerate

along the Z direction of the slice can be seen, the water saturation is mainly concentrated in the middle to the end of the core, non-homogeneity is very strong.

Oil saturation characterization. The initial state of the rock can be considered that the pores are filled with air and the whole structure is the CT value of the skeleton and pores. Then the rock samples are saturated with oil, the pores are filled with oil, and

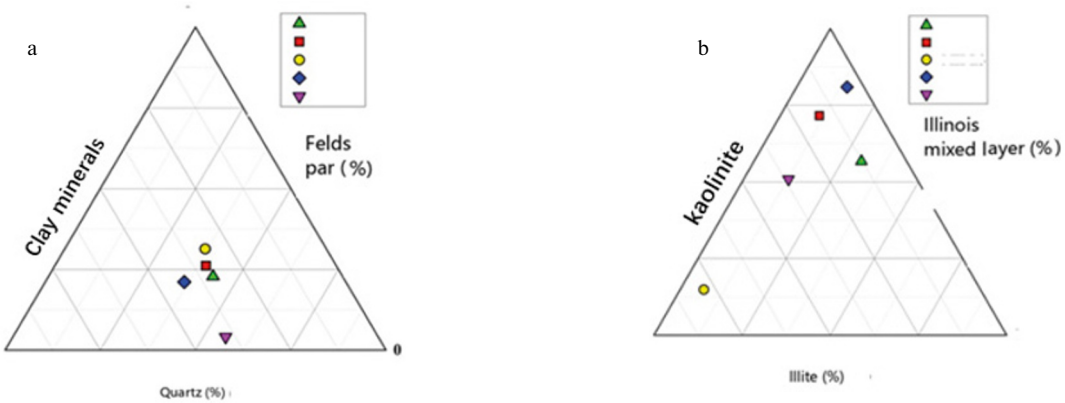

Fig. 3. Ternary diagram of mineral content of glutenite

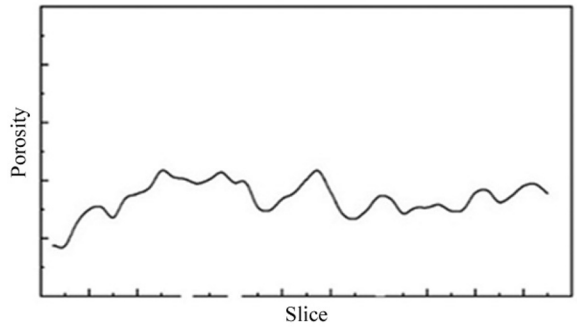

Fig. 4. Porosity slice along the way

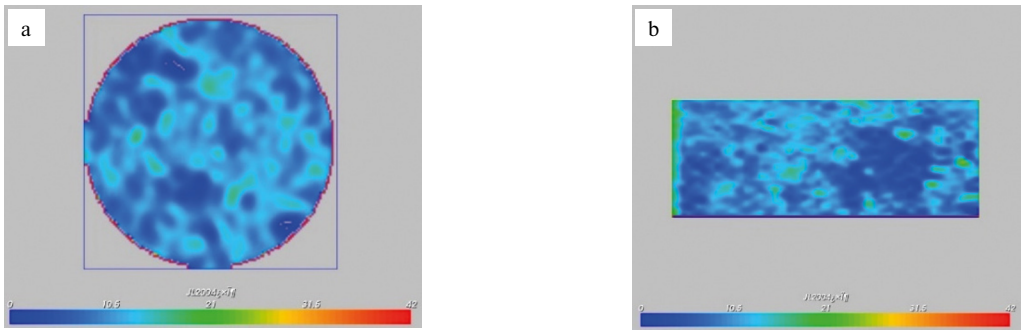

Fig. 5. Core slices in different directions. a) Transverse section; b) Axial section

the whole structure is the CT value of the skeleton and oil. Replacement of the gravel, replacement process, the pore space for the oil and water CT value of the sum, the CT value of the skeleton remains unchanged, the whole structure of the skeleton, oil and water CT value of the sum. By calculating the change of CT value, the change of oil saturation can be calculated.

As shown in **Figure 6**, at 10 minutes of water drive, the water phase is mainly concentrated in the first 1/3 of the plunger section at the injection end, the oil saturation at the first end decreases obviously, and a large amount of water is stored in the pore space at the injection end, and there is no obvious change in the oil saturation in the middle and the tail. After 1 hour of

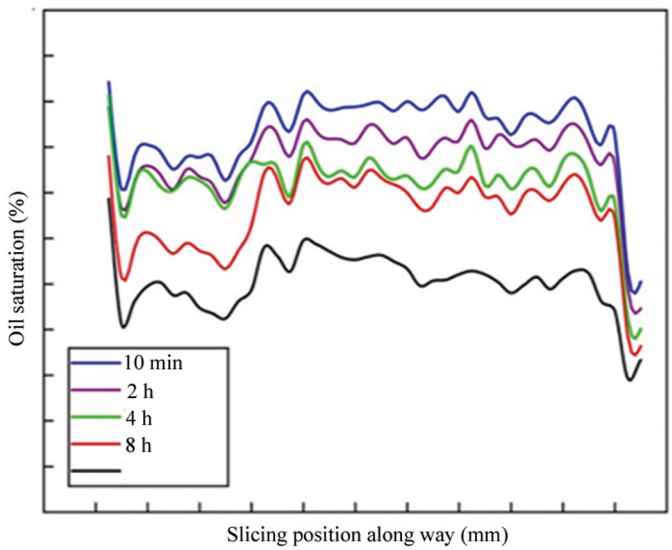

Fig. 5. Core slices in different directions. a) Transverse section; b) Axial section

displacement (Fig. 3.7), the water saturation of the plunger section 2/3 of the way from the tail end decreased significantly, the oil saturation of the plunger section 1/3 of the way from the first end did not decrease significantly, the seepage channel was completely circulated, and the oil saturation at the tail end decreased rapidly. After 4 hours of displacement (Fig.3.8), the saturation at the tail end decreased significantly, while the saturation at the first end remained unchanged. The whole pre-process is mainly dominated by the decrease of oil saturation in the tail end of the rock, which covers about 2/3 of the whole rock.

After 8 hours of replacement (Fig. 3.9), the oil saturation of the first end of the rock decreases significantly, and when the oil is discharged from the tail end, the water repulsion process is mainly concentrated in the first end, and the wave length accounts for about 1/3 of the entire length of the rock. After 16 hours of replacement (Fig. 3.10), the water saturation decreases in general, and then all the seepage channels are completed circulation, and at this time the water content reaches more than 95%. In the slices of five different replacement time periods, the blue color is the water phase, the red color represents the skeleton and filler, and the green part is the oil phase.

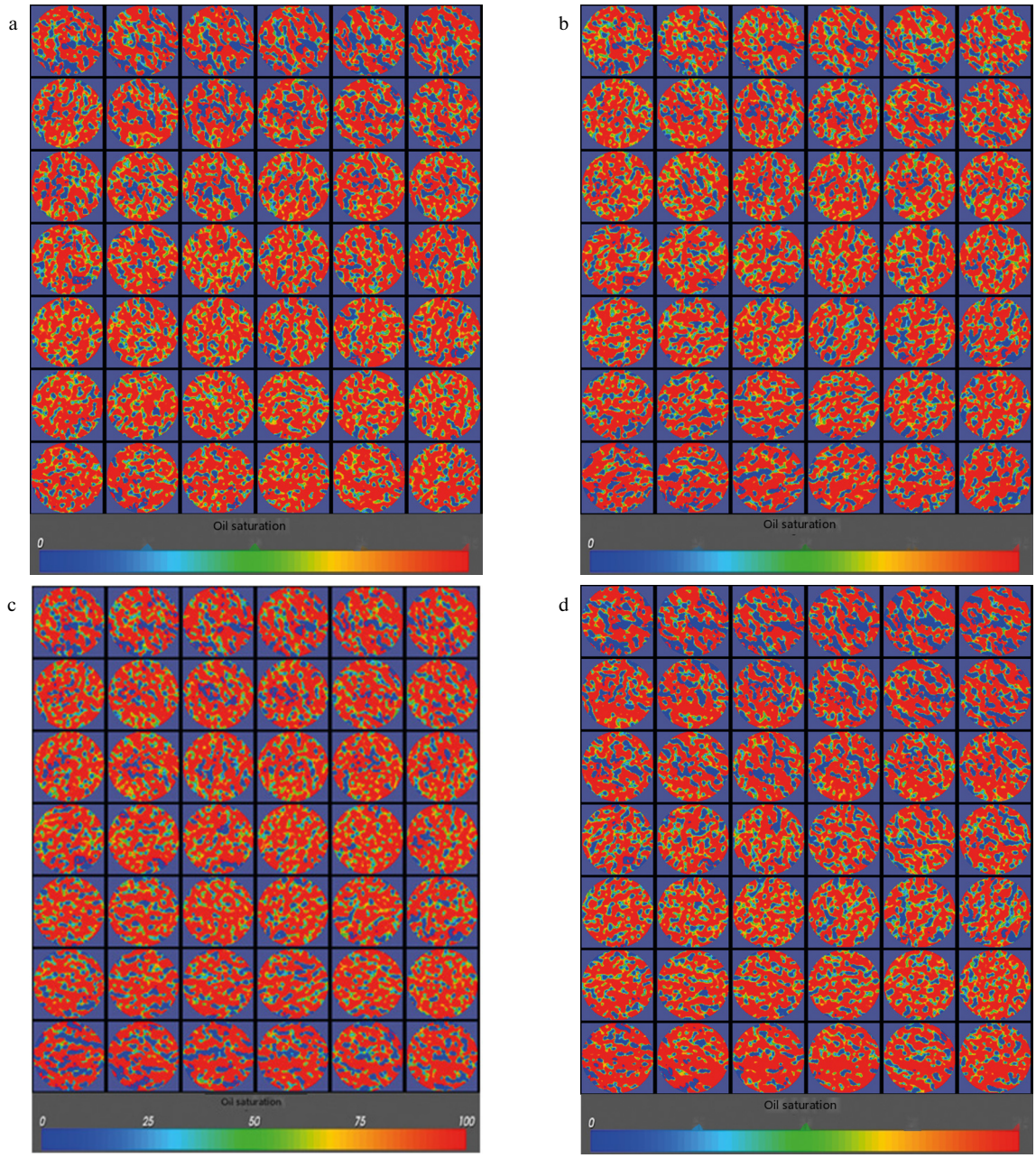

Fig. 7. Change diagram of two-phase saturation after 10 min (a), 2 h (b), 4 h (c), 8 h (d) of displacement

4. Conclusions

In this chapter, spontaneous seepage NMR experiments and CT monitoring experiments of differential pressure drive were carried out for dense conglomerates to elucidate the two-phase seepage pattern.

In the process of spontaneous seepage, the fluid circulation inside the pore space of dense gravel is high, and basically no microcracks are generated. The high content of clay minerals in contact with water causes the pore volume to increase, which improves the recovery rate of seepage. However, the strongly inhomogeneous gravel distribution increases the complexity of the seepage path, which reduces the seepage recovery rate. The gravels have higher seepage rate under the OEO boundary condition (single-cut contact seepage), but the final seepage recovery is the lowest. The confinement of the side area of the samples reduced the recovery rate under the corresponding boundary conditions. The closure of the sample side area reduces the recovery rate under the corresponding boundary condition, but the normalized recovery rate after the scaling of the sample size, porosity, permeability, fluid viscosity and surface tension in the time model is higher than that of the boundary condition with the side area not closed, and the opening of the core side can improve the recovery rate, but the degree of contribution is limited.

The non-homogeneity of the gravel is strong, which leads to the formation of dominant channels in the seepage process. In the early period of replacement, the effect of water repulsion is poor, and a large amount of water accumulates. With the growth of replacement time, a large amount of water enters into the middle of the rock sample, and the oil saturation at both ends has no obvious change. The oil saturation is lower at both ends and higher in the middle. In the late stage of replacement, the oil saturation in the middle of the sample decreases, and there is no obvious change in the oil saturation at the injection end and the output end. With the increase of the replacement time, the pore space of the whole sample is opened, and the oil saturation decreases obviously.

REFERENCES

1. Bai Zhenqiang, Wu Shenghe, Fu Zhiguo. Microscopic residual oil distribution law after polymer driving in Daqing oilfield[J]. Journal of Petroleum, 2013, 34(5): 924-931.

2. Wang Y., Song G.Q., Liu H.M., et al. Main controlling factors of shale oil enrichment in Jiyang depression[J]. Oil and Gas Geology and Recovery, 2015, 22(4): 20-25.

3. Zhang Yadong, Gao Guanghui, Liu Zhengpeng, et al. Characteristics of differential fluid storage in tight sandstone reservoirs--an example of the Triassic Yanchang Formation in the Ordos Basin[J]. Petroleum Experimental Geology, 2021, 43(06): 1024-1030.

4. Zhang S. Molecular dynamics simulation of shale oil storage characteristics in the Dongying Depression[J]. Oil and Gas Geology and Recovery, 2021, 28(5): 74-80.

5. Liu Xiong, Yan Le, Zhang Yang, et al. Analysis of factors affecting spontaneous seepage and absorption in dense sandstone reservoirs[J]. Yunnan Chemical Industry, 2021, 48(08): 55-57+71.

6. Jing Yang. Analysis of seepage and absorption mechanism of porous media and its influencing factors[J]. Yunnan Chemical Industry, 2020, 47(11): 138-140.

7. Wang Chenguang. Characteristics of spontaneous seepage and suction in tight sandstone reservoirs under different boundary conditions[J]. Journal of Xi'an Petroleum University (Natural Science Edition), 2021, 36(03): 58-65+70.

8. Zhenjie Zhang, Jianyuan Feng, Jianchao Cai, et al. Drivers of seepage and suction under different boundary conditions[J]. Computational Physics, 2021, 38(05): 513-520.

9. Schechter D. S., Denqen Z., Orr F. M. Capillary imbibition and gravity segregation in low IFT systems[C]//SPE Annual Technical Conference and Exhibition. OnePetro, 1991.

10. Li Shikui, Liu Weidong, Zhang Haiqin, et al. Experimental study of spontaneous seepage and suction drive in low-permeability reservoirs[J]. Journal of Petroleum, 2007, 28(2): 109-112.

11. Jing Yang. Experimental study on seepage and absorption of slip water fracturing in tight sandstone gas reservoir in Box 8 section of Surig gas field[J]. Yunnan Chemical Industry, 2020, 47(2): 111-112.

12. Zhou Desheng, Shi Yuhan, Li Ming, et al. Study of seepage and suction characteristics of dense sandstone based on nuclear magnetic resonance experiment[J]. Journal of Xi'an Petroleum University: Natural Science Edition, 2018, 33(2): 51-57.

13. Cai Jianchao, Yu Boming. Progress in the study of spontaneous percolation in porous media[J]. Advances in Mechanics, 2012, 42(6): 735-754.

14. Cai Jianchao. Key issues and thoughts on spontaneous percolation in porous media[J]. Computational Physics, 2021, 38(05): 505-512.

15. Lv Guoxiang, Zhang Jin, Liu Dawei, et al. Research progress of technology for improving water-driven recovery in high water-bearing oilfields[J]. Drilling Process, 2010, 33(2): 55-57.

16. Yuan Shiyi, Wang Qiang, Li Junshi, et al. Progress and prospect of gas injection enhanced recovery technology[J]. Journal of Petroleum, 2020, 41(12): 1623-1632.

17. Liu Rongquan, Yang Shuangchun, Pan Yi, et al. Progress of gas foam oil repulsion research[J]. Contemporary Chemical Industry, 2016, 45(3): 627-629.

18. Yang Liu, Wang Hengkai, Xu Huijin, et al. Experimental study on characteristics of water imbibition and ion diffusion in shale reservoirs[J]. Geoenergy Science and Engineering, 2023, 229, 212167.

19. Wu Ya-Li, Wang Cheng-Sheng, Kan Liang, et al. Characterization of high-magnitude water drive by nuclear magnetic resonance[J]. Petrochemical Applications, 2019, 38(12): 15-19.

20. Shin Zhena, Wang Xiangzeng, Kang Zhaoyu, et al. Quantitative analysis of seepage-absorption-drive-off oil recovery mechanism of typical tight oil reservoirs in Yanchang Oilfield[J]. Oil and Gas Geology and Recovery, 2018, 25(5): 99-103.

21. Deng Shiguan, Lv Weifeng, Liu Qingjie, et al. Study of oil driving mechanism in conglomerate using CT technology[J]. Petroleum Exploration and Development, 2014, 41(03): 330-335.

22. Yang Liu, Yang Duo, Zhang Mingyuan et al. Application of nano-scratch technology to identify continental shale mineral composition and distribution length of bedding interfacial transition zone - A case study of Cretaceous Qingshankou ormation in Gulong Depression, Songliao Basin, NE China, Geoenergy Science and Engineering, 2024, 234, 212674.